POLISH JOURNAL OF NATURAL SCIENCES
Abbrev.: Pol. J. Natur. Sc., Vol 34(3): 383–394, Y. 2019

EFFECT OF THE EXTERNAL ELECTRIC FIELD ON THE STRUCTURE AND REACTIVITY OF DEOXYRIBONUCLEIC ACIDS

***Józef Mazurkiewicz*[1], *Wojciech Ciesielski*[2], *Piotr Tomasik*[3], *Przemysław Jan Tomasik*[4]**

[1] ORCID: 0000-0003-1815-1572
[2] ORCID: 0000-0001-6844-348X
[3] ORCID: 0000-0003-2438-3643
[4] ORCID: 0000-0002-2061-999X
[1] Department of Chemistry and Physics
University of Agriculture in Krakow, Poland
[2] Institute of Chemistry, Environmental Protection and Biotechnology
Jan Długosz Academy in Częstochowa, Poland
[3] Nantes Nanotechnological Systems in Bolesławiec, Poland
[4] Department of Clinical Biochemistry, Collegium Medicum
Jagiellonian University in Kraków, Poland

Key words: adenine, cytosine, DNA, guanine, phosphorylated deoxyribose, thymine.

Abstract

The study of the effects of static external electric fields (EEF) on the structure of several biologically important compounds has been now extended to the structure of deoxyribonucleic acids and interactions via intermolecular hydrogen bonds in the thymine-adenine and cytosine-guanine pairs. The present study involves computations of changes in energy, and dipole moments, charge density and bond lengths of fragments of deoxyribonucleic acid in response to applied external electric fields of 0.00, 5.14, 25.70 and $51.40 \cdot 10^6$ MV cm^{-1}. The computations were performed with the help of a commercial package (HyperChem 8.0) software together with the PM3 method for optimization of the conformation of the molecules. The raise in the EEF strength to $5.14 \cdot 10^6$ MV cm^{-1} has a subtle effect on the molecular energy of the systems. On elevating the strength up to $25.70 \cdot 10^6$ MV cm^{-1} that decrease in molecular energy was more significant. EEF has a tremendous effect on their reorientation in the Cartesian system, geometry of deoxyribonucleic acid and the ability of particular bases within it to form intermolecular hydrogen bonds. Observed changes evoked by the EEF were specific for particular molecules. They resulted mainly from the polarization of the bonds and from steric deformations of the molecules. Based on the energy criterion, regardless of the EEF strength applied, the ACGT (adeniane-cytosine-guanine-thymine) fragment with *T1, C2*, *G2* and *A1* tautomers is more stable than that fragment bearing *T1, C1, G1* and *A1* tautomers. The EEF of the strength up to

Address: Piotr Tomasik, Nantes Nanotechnological Systems, Dolne Młyny 21, 57-700 Bolesławiec, Poland, e-mail: rrtomasi@cyf-kr.edu.pl

$51.40 \cdot 10^6$ MV cm^{-1} breaks neither *T-A* nor *C-G* intermolecular bonds but only influence their lengths. EEF, independent of its strength, only slightly influenced the charge density of the phosphoryl group of phosphorylated deoxyribose. A possible splitting of the bonds in that group was only slightly facilitated.

Introduction

All organisms are permanently exposed to static electric fields (SEF) in nature. Natural SEF is the highest at ground level (with electric field intensities of usually 100–150 V m^{-1}) and decreases with an increase in the distance from the ground level. Its strength depends upon temperature, humidity and the presence of ionized molecules (BERING, FEW and BENBROOKE 1998). In the environment transformed by humans, additional, artificial forms of SEF are quite common. Typically, in houses its strength does not exceed 500 V m^{-1}. However, around old types of TV sets and other high-voltage equipment it can raise up to 1 to 20 kV m^{-1}. Typical technical devices generating SEF are direct current (DC) transmission lines, cathode ray tube displays, electric trams and railways. High-voltage direct current (HVDC) transmission lines produce SEF up to the 35 kV m^{-1} (±600 kV HVDC transmission line) strength, DC motors in railway systems generate up to 0.3 kV m^{-1} inside the train, and between 10–20 kV m^{-1} at a distance of 30 cm from cathode ray tube displays. Surprisingly the strength up to 500 kV m^{-1} can be measured at the human body from static charge on clothing. SEF is well absorbed by water in the surface layers of organisms. Usually skin is efficient barrier.

Artificial SEF and electromagnetic fields are called electrosmog (BRAUNER 1996). In humans it generates problems with concentration, memory, sleeping, bad mood and fatigue. There are also links between electrosmog, Alzheimer disease and leukemia (MARSHALL and RUMANN HEIL 2017). Little is known on the influence of SEF on genetic material. Chromosomal abnormalities noted in tumor cells after a 14-day static SEF exposure (8–16 kV m^{-1}) in living mice are in contrast to common believe that SEF does not penetrate living systems and, hence, is not harmful (MARINO et al. 1974, MITCHELL et al. 1978, ARRUDA-NETO 2015, PETRI et al. 2017). Thus, a coincidence between SEF and skin benign lesions, cancer and melanoma should be taken under consideration. For this sake, artificially generated SEF stimulates a concern about its influence upon human organisms and generally on flora and fauna (NATIONAL RESEARCH COUNCIL (US),1993, VAN RONGEN et al. 2007, MARUVADA 2012,VIAN et al. 2016, PETRI et al. 2017).

In order to recognize the effect of the static external electric field (EEF) of varying strength upon the structure and reactivity of several biologi-

cally essential molecules, numerical simulations were performed. Such simulations were formerly performed for common simple molecules as water, nitrogen, carbon dioxide and ammonia (MAZURKIEWICZ and TOMASIK 2010), and biologically important molecules, that is, monosaccharides (MAZURKIEWICZ and TOMASIK 2012), alkanols (MAZURKIEWICZ and TOMASIK 2012a), porphin and metalloporhyrins (MAZURKIEWICZ and TOMASIK 2013), proteogenic amino acids (MAZURKIEWICZ and TOMASIK 2013a), selected di- (MAZURKIEWICZ and TOMASIK 2014) and tri-peptides (MAZURKIEWICZ et al. 2015), selected lipids, that is fatty acids and their glycerides (MAZURKIEWICZ et al. 2016) and complex lipids (MAZURKIEWICZ et al. 2017) and recently (MAZURKIEWICZ et al. 2018) to selected pyrimidine and purine bases. That research was stimulated by the role of electricity in the human life.

DNA is a highly charged molecule. Sudden defects of DNA like strand breaks generate SEF of quadrupole nature, and it lasting till the structure will be repaired. SEF can produce also nanochanges in DNA and/or RNA structure (JACQUEMIN et al. 2014). Recently performed computations (ARABI and MATTA 2018) showed that fields $\geq +3.60 \cdot 10^9$ V m^{-1} facilitate the mutation in the GC base pair and reduce the rectification of point mutations.

This paper presents numerical simulations performed for fragments of deoxyribonucleic acid and DNA in EEF of varying strength. In all our former studies computations were performed for EEF of 5.14, 25.70 and 51.40 MV cm^{-1}. In the latter case, in the dry air, the minimum spark gap reach over 50 m. Such drastic conditions can be followed near the lightning during a storm.

The computations were performed employing chiefly the PM3 method. However, a fragment of the presented data was obtained involving the DFT approach in order to demonstrate that both methods offer qualitatively the same tendencies in the influence of the EEF strength upon studied structures and their properties.

Computations

PM3 Computations

The HyperChem 8.0 software (HYPERCHEMRELEASE 8.0.7) was used together with the PM3 method (STEWART 1998) for optimization of the conformations of the molecules under study. Optimization was performed for molecules out of the field as well as in the presence of the field. Charge distributions, potentials and dipole moments for the molecules

placed in EEF of 5.14, 25.70 and 51.40 MV cm^{-1} were calculated. The molecules were situated along the *x*-axis. The *y*- and *z*-axes were perpendicular in plane and perpendicular to plane containing this structure, respectively. Hence the simulation was performed for molecules oriented in space relative to the applied EEFs. EEF acted along the *x*-axis.

DFT Computations

The geometry optimizations were performed for the ground state using density-functional theory (DREIZLER and GROSS 1990) DFT method with Becke's three-parameter hybrid exchange functional (BECKE 1988, 1993) with Lee-Yang-Parr gradient-corrected correlation functional (LEE et al. 1988) B3LYP and basis set 6-31G. No constraints to bonds/ angles/dihedral angles were applied in the calculations. DGauss engine in the Cache (GAUSS 1985) and GAUSSIAN 98 (FRISCH et al. 1988) was employed.

Results and Discussion

As components of DNA and RNA, pyrimidine and purine bases play a key biological role. Either ribose in DNA or deoxyribose in RNA form a chain by 3 → 6' esterification with phosphoric acid. Resulting chain with either pyrimidine or purine bases subsequently bound to the 1-position of the sugar units (Figure 1) turns into a helix.

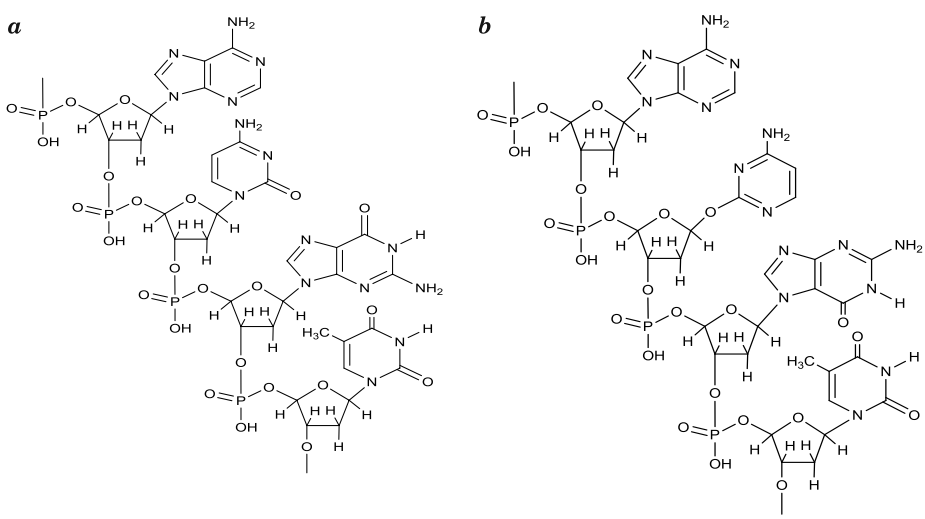

Fig. 1. A simplified fragment of the DNA chain (ACGT) with commonly accepted (*a*) and with those resulting from computations (*b*) dominating tautomers of cytosine and guanine

In the simplified structure of the *ACGT* fragment (Figure 1) commonly recognized dominating tautomers of cytosine, guanine and adenine are taken into account (Figure 1*a*). However, our recent numerical computations (MAZURKIEWICZ et al. 2018) performed for those bases revealed that when out of field, for cytosine (*a*) and guanine (*b*) dominate tautomers presented in Figure 2 . In EEF of the 5.14 MV cm^{-1} strength in cytosine also dominates tautomer (*a*) and in EEF of the 51.40 MV cm^{-1} in adenine the tautomer (*c*) dominates.

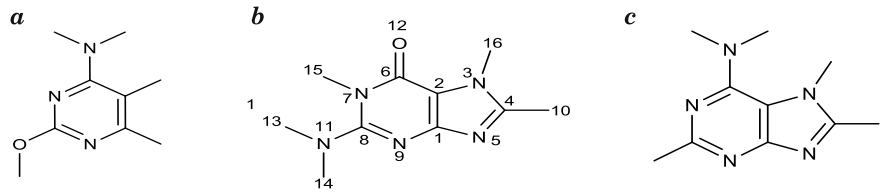

Fig. 2. Dominating tautomers of cytosine (*a*), guanine (*b*) and adenine (*c*)

These computations for the system bearing the *C1* and *G1* tautomers showed that its energy decreased in the EEF with an increase in its strength (Table 1). Simultaneously its total dipole moment considerably increased.

Table 1

Energy of the *ACGT* fragment of DNA out of EEF and in the EEF of increasing strength and changes in its dipole moment under such circumstances*

EEF strength [MV cm^{-1}]	Energy (E) [kcal mole^{-1}]	$E_I - E_0$	Dipole moment [D]			
			total	*x*-axis	*y*-axis	*z*-axis
0.00	-354361	0	18.00134	-17.25998	0.84573	-5.04242
	-357598**	0	7.49662	3.01923	5.87363	2.35492
5.14	-354369	-8	19.33981	-18.33981	-1.03399	-5.12429
	-357597**	-1	6.88824	2.39524	5.89156	2.64578
25.70	-354392	-31	28.38129	-27.92123	-1.99175	-4.68350
	-357653**	-55	19.07635	-15.92908	8.02015	6.77117
51.40	-354445	-84	47.34115	-47.93203	0.93418	0.04134
	-357680**	-82	28.69667	-26.28798	7.93017	8.33989

* If not denoted the results are for the *ACGT* fragment with *A1, C1, G1* and *T1* tautomers
** Data for the ACGT fragment carrying *A1,C2, G2* and *T1* tautomers

Simultaneously, the *C2* and *G2* tautomers incorporated into that ACGT fragment stabilized the system in terms of energy.

Dipole moment of the system bearing the *C1* and *G1* tautomers also increased with the EEF strength and regardless its value the orientation of the molecule along x-axis predominated, particularly on exposure to the EEF of 51.40 MV cm^{-1}. Replacing the *C1* and *G1* tautomers in the system

with *C2* and *G2* tautomers, respectively, resulted a considerable decrease in the total dipole moment. In contrast to the former system, that modified prefers situating mainly along the y-axis with the preference for changing orientation in the space along the *x*-axis as the EEF strength increases.

Separate computations performed for a fragment composed of two phosphorylated deoxyriboses (Figure 3) showed how EEF depending on its strength influenced the phosphoric acid moiety linking two deoxyribose units. Table 2 reveals that EEF independently of its strength only slightly influenced the charge density of the phosphoryl group. A possible splitting of the bonds in that group under the influence of EEF was only slightly facilitated.

However, the considerable polarization of the O^3-H^4 bond should be emphasized.

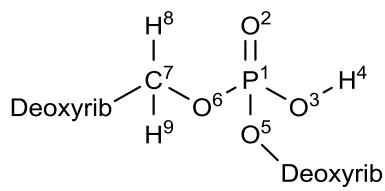

Fig. 3. Two phosphorylated deoxyriboses

Table 2

Charge density distribution in phosphorylated deoxyribose unit out of field and EEF of varying strength*

EEF strength [MV cm^{-1}]	Charge density at atoms*								
	1	2	3	4	5	6	7	8	9
0.00	2.187	-0.847	-0.630	0.245	-0.630	-0.630	0.115	0.018	0.045
5.14	2.187	-0.851	-0.628	0.246	-0.649	-0.637	0.114	0.018	0.042
25.70	2.186	-0.866	-0.627	0.251	-0.645	-0.633	0.111	0.024	0.030
51.40	2.184	-0.889	-0.628	0.263	-0.631	-0.631	0.112	0.014	0.028

* See Figure 4 for notation of particular atoms

In nature two separated helices of either DNA or RNA form a double helix stabilized by intermolecular hydrogen bonds between their *C* and *G*, as well as *T* and *A* moieties. In double helix, *T* is replaced by uracil, *U*. Computations were performed for model *C*1-*G*1 and *T*1-*A*1 as well as *C*2-*G*2 and *T*1-*A*2 pairs (Figure 4) in order to check how EEF could influence their hydrogen bonding. The results are given in Tables 3–5.

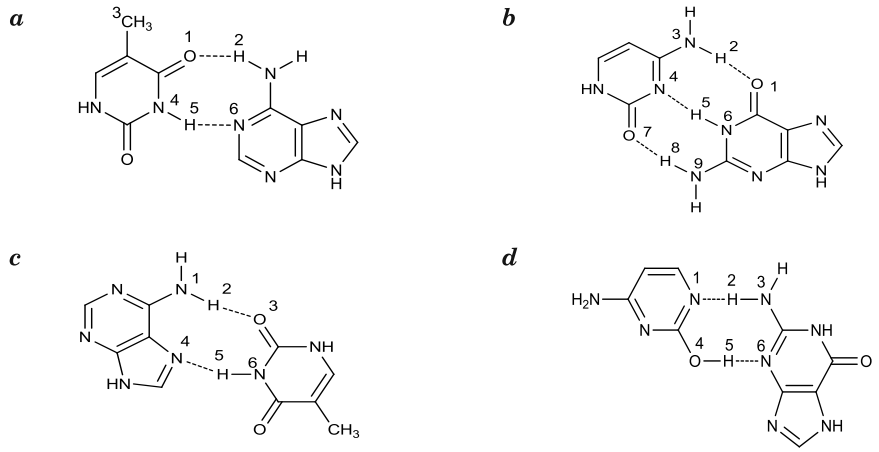

Fig. 4. Intermolecular hydrogen bonds in *T*1-*A*1 (*a*) and *C*1-*G*1 (*b*), *T*1-*A*2 (*c*) and *C*2-*G*2 (*d*) pairs

Table 3

Hydrogen bond lengths in the *T*-*A* and *C*-*G* pairs*

EEF [MV cm^{-1}]	Bonds [Å]								
	1-2	2-3	1-2 + 2-3	4-5	5-6	4-5 + 5-6	7-8	8-9	7-8 + 8-9
T-*A*									
0.00	1.8209	1.0079	2.8288	1.0356	1.7806	2.8162	–	–	–
5.14	1.8151	1.0061	2.8212	1.0341	1.7871	2.8212	–	–	–
25.70	1.8136	1.0103	2.8239	1.0302	1.8146	2.8548	–	–	–
51.40	1.8473	1.0100	2.8573	1.0324	1.8351	2.8675	–	–	–
–	*1.0082*	*1.8064*	*2.8146*	*0.9937*	*2.7478*	*3.7415*			
C-*G*									
0.00	1.8643	0.9692	2.8335	1.0697	1.6347	2.7044	1.0462	1.5551	2.6093
	1.7342	**1.0051**	**2.7393**	**1.0562**	**1.5215**	**2.5777**	**0.9922**	**1.6028**	**2.5950**
	1.8090	*1.0212*	*2.8302*	*0.9766*	*1.7836*	*2.7602*	–	–	–
	1.8025	***0.9965***	***2.7990***	***0.9995***	***1.6985***	***2.6980***	–	–	–
5.14	1.8597	0.9697	2.8294	1.0675	1.6404	2.7079	1.0375	1.5755	2.6130
	1.8052	*1.0211*	*2.8263*	*0.9766*	*1.7860*	*2.9626*			
25.70	1.8443	0.9727	2.8170	1.0580	1.6675	2.7255	1.0166	1.6323	2.6489
	1.7920	*1.0212*	*2.8132*	*0.9765*	*1.7938*	*2.7705*			
51.40	1.8254	0.9773	2.8027	1.0476	1.7033	2.7509	1.0012	1.6866	2.6378
	1.7196	*1.0359*	*2.7555*	*0.9695*	*1.8515*	*2.8210*	–	–	–

* Upper values are for the *C*1-*G*1 and *T*1-*A*1 systems whereas the lower values in italics are for *C*2-*G*2 and *T*1-*A*2 systems, respectively, calculated involving PM3 method. Figures in bold are calculated involving the DFT approach

Table 4

Charge density distribution on the atoms directly involved in the intermolecular bonds formation in the *T*1-*A*1 and *T*1-*A*2 systems

EEF [MV cm^{-1}]	Atoms*					
	1	2	3	4	5	6
0.00	-0.406	0.119	0.119	-0.073	0.197	-0.263
5.14	-0.408	0.123	0.128	-0.073	0.194	-0.264
25.70	-0.415	0.127	0.108	-0.078	0.182	-0.256
51.40**	-0.414 *-0.144*	0.102 *0.127*	0.052 *-0.510*	-0.094 *0.345*	0.183 0.098	-0.274 *0.079*

* See Figure 5*a* for the atoms notation for the *T*1-*A*1 system and Figure 5*c* for the *T*1-*A*2 system
** Lower cases in italics relate to the charge density distribution in the *T*1-*A*2 system

Table 5

Charge density distribution on the atoms directly involved in the intermolecular bonds formation in the *C*1-*G*1 and *C*2-*G*2 systems*

EEF [MV cm^{-1}]	Atoms**								
	1	2	3	4	5	6	7	8	9
0.00	-0.126 *-0.280*	0.239 *0.143*	-0.241 *0.017*	0.040 *-0.223*	0.237 *0.272*	-0.357 *-0.172*	-0.311	0.322	-0.352
5.14	-0.130 *-0.279*	0.241 *0.145*	-0.243 *0.025*	0.044 *-0.227*	0.235 *0.272*	-0.357 *-0.180*	-0.304	0.322	-0.350
25.70	-0.150 *-0.276*	0.251 *0.152*	-0.250 *0.057*	0.055 *-0.243*	0.227 *0.071*	-0.356 *-0.213*	-0.286	0.319	-0.333
51.40**	-0.181 *-0.318*	0.265 *0.191*	-0.260 *0.118*	0.062 *-0.248*	0.215 *0.247*	-0.340 *-0.226*	-0.267	0.311	-0.296

* See Figure 5*b* for the atoms notation in the *C*1-*G*1 system and Figure 5*c* in the *C*2-*G*2 system
** Lower cases in italics relate to the charge density distribution in the *C*2-*G*2 system

*T*1 with A1 form the pair involving two hydrogen bonds (Figure 4*a*). EEF of 5.14 MV cm^{-1} decreased the length of the C = O….H-NH (1-2) bond and, simultaneously, increased the length of the N-H…N(aza) (5-6) bond. These changes were accompanied by shortening the length of the both H-N valence (2-3 and 4-5) bonds to a such extent that total distance between two bases was reduced. The original planar structure of the pair of those bases was retained. The application of the EEF of 25.70 MV cm^{-1} still reduced the length of the 1-2 bond but increased the length of the 2-3 bond. The bonds 4-5 and 5-6 shortened and extended, respectively. Insight in the three dimensional structure of that pair revealed that it was bent to form a structure of a shallow saddle (Figure 5a). At EEF of 51.40 MV cm^{-1} only the 2-3 bond slightly shortened and the other bonds considerably expanded as the deformation of the saddle structure progressed (Figure 5*b*).

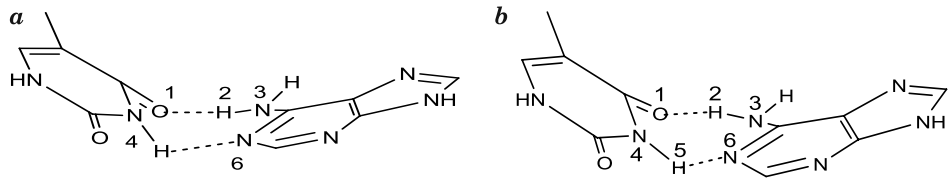

Fig. 5. The saddle structure of the *T*1-*A*1 pair in the EEF of the 25.70 MV cm^{-1} (*a*) and 51.40 MV cm^{-1} (*b*) strength

As shown in our recent paper (MAZURKIEWICZ et al. 2018), in the EEF field of the 51.40 MV cm^{-1} strength the *A*1 tautomer lost its dominating role in favor of the *A*2 tautomer. Computations performed for the *T*1-*A*2 pair (Table 3) revealed a considerable decrease in the 1-2 and 4-5 bond length and, simultaneously, elongation of the 2-3 and 5-6 bonds to a such extent that the sum of the lengths of the 1-2 and 2-3 bonds was to that computed for the *T*1-*A*1 pair and the sum of the 4–5 and 5-6 bond lengths was significantly higher. In contrast to the behavior of *T*1-*A*1 pair in the EEF of that strength, the *T*1-*A*2 pair although, reoriented in the Cartesian system, remained planar.

The formation of the *C*1-*G*1 pair involved three hydrogen bonds (Figure 4*b*). The EEF strength increase was followed by elongation of the = N-H….O = C (2-3) and shortening of both the N(aza)… H-N (4-5) and C = O….H-NH (7-8) hydrogen bonds. Simultaneously, the HN-H (1-2), N(aza)-H (5-6) and HN-H (8-9) valence bonds shortened, expanded and expanded, respectively. In that manner the EEF caused shortening of the 1–3 distance and elongation of the 4–6 and 7–9 distances. Independently of the EEF strength the *C*1-*G*1 pair remained planar.

The replacing of the *C*1 and *G*1 tautomers in the *ACGT* system with the *C*2 and *G*2 tautomers resulted, first of all, in reduction of the intermolecular hydrogen bonds from 3 to two (Figure 5). Compared to the ACGT fragment with the *C*1 and *G*1 tautomers there was a shortening of the 1-2 and 4-5 bonds and elongation of the 2-3 and 5-6 bonds, respectively. The sum of the 1-2 + 2-3 bonds was shorter, whereas the sum of the 4-5 + 5-6 bonds was longer.

Insight in Table 4 revealed that in the *T*1-*A*1 pair the EEF increasing its strength increased slightly the negative charge density on the carbonyl oxygen atom of thymine as well as on the aza atom of the pyrimidine part of adenine. The charge density on both hydrogen atoms increased with the strength of EEF but these changes varied on a chimeric manner because of the deformation of the structure from planar towards a saddle-like (Figure 5) and accompanying changes in the bond lengths (Table 3). Such deformation caused a twist of the exocyclic amino group of the adenine

moiety partly cancelling the resonance interaction with the π-orbital of adenine. It explained a relatively large decrease in the positive charge density on the nitrogen atom of that group. In the *T*1-*A*2 system in the EEF of the 51.40 MV cm^{-1} strength, the negative charge density shifted from the aza atom 6 to the exocyclic amino group nitrogen atom 3.

Inspection of data in Table 5 similarly revealed that an increase in the EEF strength increased the ability of the carbonyl oxygen atoms of *C*1 and *G*1 favoring the hydrogen bond formation irregularly influenced the positive charge density of the hydrogen atoms participating in the formation of those hydrogen bonds.

In the *C*1-*G*1 system, the negative charge density on the carbonyl oxygen atom (O7) in the *C*1 moiety decreased with the EEF strength whereas, simultaneously, very small positive charge density on the *C*1 aza-atom N4 slightly increased. The nitrogen atom of the exocyclic amino group of *C*1 also carried considerable negative charge density which increased with the EEF strength. The latter effect was responsible for an increase in the positive charge density of the hydrogen atom participating in the hydrogen bonding to the G1 carbonyl group oxygen atom (O3) of *G*1. The aza-atom, N6, and the nitrogen atom of the exocyclic amino group (N9) of *G*1 carried considerable negative charge density, both decreasing as the EEF strength increased. Simultaneously, decreased the positive charge density on the hydrogen bonds forming hydrogen atoms, H5 and H8.

In the *C*2-*G*2 system the negative charge density on the N1 atom was much higher and simultaneously, the negative charge density on the N6 atom turned lower than that in the *C*1-*G*1 system. The charge density on the O3 atom turned from negative in the *C*1-*G*1 system into positive and the positive charge density on the N4 atom in the latter system turned into considerably negative and increasing with the EEF strength.

Conclusions

Observed changes evoked by the EEF are specific for particular molecules. They results mainly from the polarization of the bonds and from steric deformations of the molecules. Based on the energy criterion regardless the EEF strength applied, the ACGT fragment with *T*1, *C*2, *G*2 and *A*1 tautomers is more stable than that fragment bearing *T*1, *C*1, *G*1 and *A*1 tautomers. That fragment with the *T*1, *C*2, *G*2 and *A*1 bases is less polar than that commonly considered correct fragment with *T*1, *C*1, *G*1 and *A*1 tautomers. The EEF of the strength up to 51.40 MV cm^{-1} breaks neither T-A nor C-G intermolecular bonds but only influences their lengths.

Solely, in case of *T*1-*A*1 pair the 25.70 and 51.40 MV cm^{-1} EEF deteriorates the planarity of the system. EEF independently of its strength only slightly influences the charge density of the phosphoryl group of phosphorylated deoxyribose. A possible splitting of the bonds in that group is only slightly facilitated.

Accepted for print 18.07.2019

References

ARABI A.A., MATTA C.F. 2018. *Effects of intense electric fields on the double proton transfer in the Wattson – Crick guanine – cytosine base pair*. J. Phys. Chem. B, 122: 8631–8641.

ARRUDA-NETO J.D.T. 2015. *Sensing of DNA damage, instantly activation of repairing proteins and radio sensitizers. A biophysical model*. MOJ Proteomics Bioinform., 2(5): 165.

BECKE A.D. 1988. *Density-functional exchange-enery approximation with correct asymptotic behavior*. Phys. Rev. A, 38: 3098–3100.

BECKE A.D. 1993. *Density-functional thermochemistry*. III. *The role of exact exchange*. J. Chem. Phys., 98: 5648–5662.

BERING E.A. III, FEW A.A., BENBROOKE J.R. 1998. *The global electric current*. Phys. Today, 51(10): 24.

BRAUNER C. 1996. *Electrosmog – a phantom risk*, http://www.emfandhealth.com/Swiss-ReElectrosmog.pdf, access: 15.03.2019.

DREIZLER M.R., GROSS E.K.U. 1990. *Density functional theory*. Springer, Heidelberg.

FRISCH M.J. et al., 1998. *GAUSSIAN 98*, Gaussian, Inc., Pittsburgh, PA. Gauss, d. 4.1 in CAChe 7.5.0.85 by FUJITSU.

HYPERCHEMRELEASE 8.0.7 *Molecular Modeling System*.

JACQUEMIN D., ZUNIGA J., REQUENA A., CERON-CARRASCO J.P. 2014. *Assessing the importance of proton transfer reactions in DNA*. Acc. Chem. Res., 47: 2467–2474.

LEE C., YANG W., PARR R.G. 1988. *Development of the Colle-Salvetti correlation-energy formula into a functional of the electron density*. Phys. Rev. B, 37: 785–789.

MARINO A.A., BERGER T.J., MITCHELL J.T., DUHACEK B.A., BECKER R.O. 1974. *Electric field effects in selected biologic systems*. Ann. N. Y. Acad. Sci., 238: 436–444.

MARSHALL T.G., RUMANN HEIL T.J. 2017. *Electrosmog and autoimmune diseases*. Immunol. Res., 65: 129–135.

MARUVADA P.S. 2012. *Electric field and ion current environment of HVdc transmission lines: Comparison of calculations and measurements*. IEEE Trans. Power Del., 27: 401–410.

MAZURKIEWICZ J., KOŁOCZEK H., TOMASIK P. 2015. *Effect of the external electric field on selected tripeptides*. Amino Acids, 47: 1399–1408.

MAZURKIEWICZ J., KOŁOCZEK H., TOMASIK P. 2016. *Effect of external electric field on fatty acids and their glycerides*. Curr. Phys. Chem., 6: 164–178.

MAZURKIEWICZ J., KOŁOCZEK H., TOMASIK P. 2017. *Effect of external electric field on model complex lipids*. Curr. Phys. Chem., 7: 71–80.

MAZURKIEWICZ J., TOMASIK P. 2010. *Contribution to understanding weak electrical phenomena*. Natur. Sci., 2: 1195–1202.

MAZURKIEWICZ J., TOMASIK P. 2012. *Effect of external electric field upon charge distribution, energy and dipole moment of selected monosaccharide molecules*. Natur. Sci., 4: 278–285.

MAZURKIEWICZ J., TOMASIK P. 2012a. *Effect of external electric field upon lower alkanols*. Adv. Natur. Sci., 5(4): 28–35.

MAZURKIEWICZ J., TOMASIK P. 2013. *Effect of external electric field to porphin and selected metalloporphyrin systems*. Compl. Alter, Med. Sci., 1: 13–21.

MAZURKIEWICZ J., TOMASIK P. 2013a. *Effect of external electric field on selected proteogenic amino acids*. Adv. Natur. Sci. (Canada), 6(1): 1–16.

MAZURKIEWICZ J., TOMASIK P. 2014. *Effect of external electric field upon selected dipeptides*. Adv. Natur. Sci. (Canada), 7(1): 6–11.

MAZURKIEWICZ J., TOMASIK P., CIESIELSKI W. 2018. *Effect of the external electric field on the structure and reactivity of selected pyrimidine and purine bases*. Curr. Phys. Chem., 8: 1–16.

MITCHELL J.T., MARINO A.A., BERGER T.J., BECKER R.O. 1978. *Effect of electrostatic fields in the chromosomes of Ehrlich ascites tumor cells exposed in vivo*. Physiol. Chem. Phys., 10: 79–85.

NATIONAL RESEARCH COUNCIL (US) 1993. *Committee on Assessment of the Possible Health Effects of Ground Wave Emergency Network (GWEN). Assessment of the Possible Health Effects of Ground Wave Emergency Network*. Washington (DC): National Academies Press (US).

PETRI A.K., SCHMIEDCHEN K., STUNDER D., DECHENT D., KRAUS T., BAILEY W.H., DRIESSEN S. 2017. *Biological effects of exposure to static electric fields in humans and vertebrates: a systematic review*. Environ. Health, 16: 41.

STEWART J.J.P. 1998. *Encyclopedia of Computational Chemistry*. J. Wiley. New York.

VAN RONGEN E., SAUNDERS R.D., VAN DEVENTER E.T., REACHOLI M.H. 2007. *Static fields: biological effects and mechanisms relevant to exposure limits*. Health Phys., 92: 584–90.

VIAN A., DAVIES E., GENDRAUD M., BONNET P. 2016. *Plant responses to high frequency electromagnetic fields*. BioMed Res. Int., Article ID 1830262.